

## Pt-Shell Nanowires for Fuel Cell Electrodes

James CM Li\*

Materials Science Program, Department of Mechanical Engineering, University of Rochester, Rochester, New York, USA

### Abstract

Gibbs idea of surface excess is reexamined to discover that the surface excess is not the same as surface enrichment. This finding could help us design Pt shell nanowires for fuel cell electrodes which should have the best performance than any other kinds of Pt catalysts. All the reasons behind this possibility are collected and discussed. It is hoped that this analysis will convince you to make such wires as fuel cell electrodes.

**Keywords:** Pt-shell nanowires; Fuel cell electrodes; Gibbs surface excess; Surface enrichment; Fuel cell cars; Self driving cars; Pt price

### Introduction

As analyzed by Ugurlu and Oztuna [1], fuel cells definitely can be used in automobiles. In fact the Toyota Mirai and Hyundai ix35 FCEV are already fuel cell cars. They can be driven 250 miles between fueling and the fueling takes only about 5 minutes. Currently \$1 worth of hydrogen can drive 146 miles while \$1 worth of gasoline can only drive 10 miles. The source of hydrogen is unlimited but gasoline will one day be gone. With hydrogen the exhaust is only water, no pollution of air as with gasoline. Hence fuel cells are the future for ground transportation.

In a fuel cell, hydrogen flows at one electrode and air flows at the other. With a catalyst the hydrogen ionizes into  $H^+$  and an electron which flows through the external circuit to the other side. The  $H^+$  diffuses through a PEM (Proton Exchange Membrane) to the other side and reacts with oxygen and an electron to form water. The second catalytic reaction is 6 orders slower than the first catalytic reaction.

The catalyst is Pt and the price of Pt can increase as much as 4% a day. If we produce more fuel cells, the price of Pt will increase rapidly. Zhu et al. [2] found a correlation between oil prices and Pt prices. They did not know why. But this is probably the reason. Luckily we need Pt only on the surface. The question is how to make a catalyst with Pt only on the surface. To increase the surface/volume ratio, we have been using Pt nanoparticles which need a support structure. The support is usually carbon. But the adhesion between Pt and C is not so good and the Pt particles can agglomerate and grow. The carbon can be oxidized also. We are looking into the self-supporting nanowires. The question is whether we can make Ni (or other metal) nanowires with only one atomic layer of Pt on the surface. The radius of a Pt atom is 135 pm and the atomic weight is 195 so a close packed layer of Pt atoms is 5 mg per square meter area, the lowest possible Pt loading achievable. This paper is to try to shed some light on this question. We are going to try to make it. You should try it too.

### Gibbs Surface Excess

Gibbs started with two homogeneous phases 1 and 2 and then let them touch each other to form an interface. Consider phase 1 of energy  $U_1$ , entropy  $S_1$ , volume  $V_1$ , chemical components  $n_{i1}$  ( $i=1$  to  $c$ ,  $c$  being the number of components):

$$dU_1 = TdS_1 - PdV_1 + \sum_{i=1}^c \mu_i dn_{i1} \quad (1)$$

This equation just says for phase 1 at constant temperature  $T$ , pressure  $P$  and all the chemical potentials  $\mu_i$  ( $i=1$  to  $c$ ) the reversible heat absorbed is  $TdS_1$ , the reversible mechanical work done is  $PdV_1$

and the reversible chemical work is  $\mu_i dn_{i1}$  ( $i=1$  to  $c$ ) by diffusing in the component  $i$ . Similarly for phase 2:

$$dU_2 = TdS_2 - PdV_2 + \sum_{i=1}^c \mu_i dn_{i2} \quad (2)$$

Now at the same temperature, pressure and all the chemical potentials, combine the two phases to form an interface. All the energy, entropy, volume, and the chemical components may change. Gibbs defined them as excess quantities due to the interface: Let  $U$ ,  $S$ ,  $V$  and  $n_i$  be the total energy, entropy, volume and the number of moles of component  $i$  of the combined system:

$$\text{Excess energy } U_{xs} = U - U_1 - U_2 \quad (3)$$

$$\text{Excess entropy } S_{xs} = S - S_1 - S_2 \quad (4)$$

$$\text{Excess volume } V_{xs} = V - V_1 - V_2 \quad (5)$$

$$\text{Excess } i^{\text{th}} \text{ component } n_{ixs} = n_{i1} - n_{i2} \quad (6)$$

These excess quantities may be negative. The system now also has an interface of area  $A$  and energy  $\gamma$  per unit area.

So for the combined system

$$dU = TdS - PdV + \gamma dA + \sum_{i=1}^c \mu_i dn_i \quad (7)$$

$$\text{Hence } dU_{xs} = TdS_{xs} - PdV_{xs} + \gamma dA + \sum_{i=1}^c \mu_i dn_{ixs} \quad (8)$$

As you may remember from your thermodynamics course, Gibbs integrated this equation by adding small quantities together into the big system at the same temperature, pressure, and all the chemical potentials. So,

$$U_{xs} = TS_{xs} - PV_{xs} + \gamma A + \sum_{i=1}^c \mu_i n_{ixs} \quad (9)$$

He then differentiated this equation and compared with eqn. (8) to obtain:

$$S_{xs} dT - V_{xs} dP + Ad\gamma + \sum_{i=1}^c n_i d\mu_i = 0 \quad (10)$$

**\*Corresponding author:** James CMLi, Professor Emeritus, Department of Mechanical Engineering, Materials Science Program, University of Rochester, Rochester, New York, USA, Tel: (585) 275-4038; Fax: (585) 256-2509; E-mail: [li@me.rochester.edu](mailto:li@me.rochester.edu)

Received May 06, 2017; Accepted May 16, 2017; Published May 26, 2017

**Citation:** Li JCM (2017) Pt-Shell Nanowires for Fuel Cell Electrodes. J Material Sci Eng 6: 337. doi: [10.4172/2169-0022.1000337](https://doi.org/10.4172/2169-0022.1000337)

**Copyright:** © 2017 Li JCM. This is an open-access article distributed under the terms of the Creative Commons Attribution License, which permits unrestricted use, distribution, and reproduction in any medium, provided the original author and source are credited.

At constant temperature, pressure and the chemical potential of all other components, the surface excess of component  $i$  is:

$$\frac{n_{xs}}{A} = - \left( \frac{\partial \gamma}{\partial \mu_i} \right)_{T,P,\mu_j} \quad (11)$$

Which is the famous Gibbs adsorption equation. It is applicable to interfaces, grain boundaries and free surfaces.

### Surface Excess and Surface Enrichment

While thermodynamics is never wrong, the prediction may not be exactly what you expected. Let us look at some of the PtNi alloys. Gauthier et al. [3,4] studied the {111} surface of 50-50 NiPt alloy. They found the surface layer contains  $88 \pm 2\%$  Pt, the second layer  $9 \pm 5\%$  Pt, the 3<sup>rd</sup> layer  $65 \pm 10\%$  Pt and the 4<sup>th</sup> layer and inside  $50\%$  Pt. Since they started with  $50\%$  Pt and the bulk is  $50\%$  Pt, the three surface layers averaged  $54 \pm 7\%$  Pt so the surface excess was  $12 \pm 7\%$  Pt if concentrated on the surface. Yet there was actually strong surface enrichment of Pt ( $88\%$ ). For the {111} surface of 50-50 NiPt alloy Van et al. [5] also found Pt enrichment on the surface. The Gibbs eqn. (11) predicts only the surface excess, not the surface enrichment. But the catalytic properties depend on the surface enrichment, not the surface excess.

For the {111} surface of an 22-78 NiPt alloy, Gauthier et al. [3,4] found the first layer  $1 \pm 1\%$  Ni, the second layer  $70 \pm 5\%$  Ni, the 3<sup>rd</sup> layer  $13 \pm 10\%$  Ni and the 4<sup>th</sup> layer and inside  $22\%$  Ni. So the surface excess is  $18 \pm 6\%$  Ni but the surface enrichment is  $99 \pm 1\%$  Pt. Based on the surface excess, this alloy may not be a good catalyst. But based on the surface enrichment, it is an excellent catalyst.

Similar results were found by computer simulation as reported by Wang et al. [6]. At 600 K, a nano particle (2 to 5 nm) of 25-75 Ni-Pt alloys has Pt strongly enriched on the surface layer and the third layer and the Ni enriched on the second layer. For a nano particle of 25-75 Re-Pt alloys, a nearly pure Pt shell surrounds a more uniform Pt-Re core. For a nano particle of 20-80 Mo-Pt alloys, the facets are fully occupied by Pt atoms, the Mo atoms are at the edges and vertices. The amount of Pt atoms on the surface increases with the size of the particle. So when it is a flat surface it will be pure Pt.

Experimentally by using LEIS (Low Energy Ion Scattering) in the same system  $Pt_{75}Ni_{25}$ , Stamenkovic et al. [7] found pure Pt on all 3 surfaces, (100), (110) and {111}. Their CTR (Crystal Truncation Rods) analysis for the {111} surface showed the second layer to consist of  $45\%$  Pt, the third layer  $82\%$  Pt and the fourth layer and inside were normal ( $75\%$  Pt). Since the average of the first 3 layers was about  $75\%$  Pt, there was no surface excess yet there was strong surface enrichment of Pt ( $100\%$ ).

Gallego et al. [8] deposited Mn on Pt {111} by evaporation and did prolonged annealing at 950 K. LEED analysis showed first layer  $100 \pm 1\%$  Pt, 2<sup>nd</sup> layer  $75 \pm 4\%$  Pt, 3<sup>rd</sup> layer  $100 \pm 10\%$  Pt, 4<sup>th</sup> layer  $75 \pm 10\%$  Pt and 5<sup>th</sup> layer and inside  $100\%$  Pt. So the surface excess is  $50 \pm 8\%$  Mn but the surface enrichment is  $100 \pm 1\%$  Pt. The surface Pt atoms have the ability to push Mn atoms inside even though Mn atoms were coated on the Pt surface.

### Some Properties of Pt Shells

Shui et al. [9] made  $PtNi_5$  nanowires by electro spinning and then treated in 0.001 M sulfuric acid for 8 minutes and heated to  $60^\circ\text{C}$  for 4 minutes to remove the Ni atoms and Ni oxides on the surface. Then the nanowires were cleaned several times in deionized water and ethanol

before they were heat treated in a hydrogen (5 vol%) argon (95 vol%) mixture at  $300^\circ\text{C}$  for 15 hours to allow Pt atoms to reach the surface to replace Ni atoms. Sure enough the Pt atoms can protect Ni in hot ( $60^\circ\text{C}$ ) 1 M sulfuric acid for hours.

Even for an alloy with 90% Ni, Tammermann et al. [10] and Gauthier et al. [11] still reported Pt enrichment on the surface. Hebenstreit et al. [12] suspected that Pt atoms on the (100) surface tend to be reconstructed into a close-packed surface layer.

For Ni-core Pt-shell nanoparticles of about 7.5 nm size, Godinez-Salomon et al. [13] made Ni core by colloidal reduction of  $NiCl_2$  with  $NaBH_4$  and coated with Pt by subsequent reduction of  $H_2PtCl_6$ . Cyclic voltammetry on thin film rotating disk electrode revealed that these particles had a more than twice enhanced catalytic activity than Pt nanoparticles synthesized by the same way.

Pt-skin surfaces were fabricated on Pt-Ni nanoparticles (2-3 nm) by Jung et al. [14] by using chemical deposition. They found that the chemically tuned Pt skin had a higher Pt coordination number and surface crystallinity which resulted in better oxygen reduction reaction activity and durability compared to the Pt-skin formed by heat annealing.

Pt-shell Ni-core nanoparticles supported on C were prepared by Kang et al. [15] with either an amorphous or crystalline Ni core while the thickness and structure of the Pt shell were similar. They compared the methanol oxidation activities by using cyclic voltammetry and chrono-amperometry and found that the amorphous core had better performance. Ni nanowires can be made by electro-spinning [9,16] and these wires can be made amorphous by straining [17].

Serra et al. [18] made mesoporous CoNi and Pt Nano rods by electrochemical synthesis and then coated the mesoporous CoNi Nano rods with a layer of Pt shell by interfacial replacement reaction. They found the later was better than the mesoporous pure Pt Nano rods. In fact they found the best ones were obtained from the water-in-ionic liquid micro emulsion which gave a mass activity of 1.3 A/mgPt.

From these considerations we suspect that Pt can protect a pure Ni wire by depositing on the surface.

### Stability of the Surface Layer

Recently, Tao et al. [19] observed compositional changes near the surface of a nanoparticle for a free surface (in vacuum) and for surfaces in different environments. So the surface layer is the most important part of the surface which is affected by the environment and can be treated as a thermodynamic phase in equilibrium with the bulk and with the environment. The Gibbs equation of state and the associated Helmholtz and Gibbs free energies are:

$$dU_s = TdS_s - PdV_s + \gamma_s dA_s + \sum_i \mu_{is} dn_{is} \quad (7.1)$$

$$dF_s = d(U_s - TS_s) = -S_s dT - PdV_s + \gamma_s dA_s + \sum_i \mu_{is} dn_{is} \quad (8.1)$$

$$dG_s = d(U_s - TS_s + PV_s) = -S_s dT + V_s dP + \gamma_s dA_s + \sum_i \mu_{is} dn_{is} \quad (9.1)$$

Unlike the Gibbs excess quantities which belong to the geometric surface, the surface quantities here are for the surface layer atoms including the surface energy  $\gamma_s$  which is not the usual surface energy but the energy for the surface layer atoms. At constant temperature, pressure, surface energy and all the chemical potentials, eqn. (7.1) can be integrated by putting small systems together and give:

$$U_s = TS_s - PV_s + \gamma_s A_s + \sum_i \mu_{is} n_{is} \quad (10.1)$$

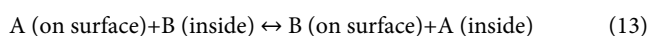
Which can be differentiated and compared with eqn. (7.1) to give:

$$A_s d\gamma_s = -S_s dT + V_s dP - \sum_i n_{is} d\mu_{is} \quad (11.1)$$

At constant temperature and pressure, the surface composition still can be found from the following equation:

$$\frac{n_{is}}{A_s} = - \left( \frac{\partial \gamma_s}{\partial \mu_{is}} \right)_{T,P,\mu_{js}} \quad (12)$$

but this is no longer the Gibbs adsorption equation since  $\gamma_s$  is not the usual surface energy and  $n_{is}$  is no longer the surface excess quantity. However now  $n_{is}$  is the real surface composition. So the surface layer is like another phase (a homogeneous part) in equilibrium with the rest of the system. The equilibrium with the interior could be an exchange equilibrium in a substitutional binary alloy of A and B such as Pt-Ni:



This exchange equilibrium can be described by:

$$\mu_{AS} + \mu_B = \mu_{BS} + \mu_A \text{ or } \mu_{AS} - \mu_{BS} = \mu_A - \mu_B \quad (14)$$

So the difference between chemical potentials of any two components is a constant throughout the system.

At constant temperature, pressure and the area of the surface layer, eqn. (9) can be integrated by adding up small systems and then differentiated to compare with eqn. (9) to obtain the Gibbs-Duhem type equation:

$$\sum_i n_{is} d\mu_{is} = 0 \quad (15)$$

For any changes of surface composition, for a binary alloy A and B, this equation can be re-arranged into:

$$x_{BS} = \frac{n_{BS}}{n_{BS} + n_{AS}} = \left[ \frac{\partial \mu_{AS}}{\partial (\mu_{AS} - \mu_{BS})} \right]_{T,P,A} = \left[ \frac{\partial \mu_{AS}}{\partial (\mu_A - \mu_B)} \right]_{T,P,A} \quad (16)$$

Where  $\mu_A$  and  $\mu_B$  are the chemical potentials for A and B in the bulk, respectively. So by changing the bulk alloy composition and examining the effect on the surface composition, it is possible to calculate the change of chemical potentials on the surface.

However, it is possible that A prefers to stay on the surface and B has zero solubility in the surface layer so that eqn. (13) is an inequality:



This inequality can be described by:

$$\mu_{BS} + \mu_{A1} > \mu_{AS} + \mu_{B1} \text{ or } \mu_{AS} - \mu_{BS} < \mu_{A1} - \mu_{B1} \quad (18)$$

Then the surface layer may not respond to the change of bulk composition. It is possible that for Pt-Ni alloy, the Pt surface layer is a stable layer obeying the inequalities represented by eqn. (18).

However, the surface layer may be in equilibrium with the surroundings such as the fluid in contact with the surface. If C is such a component, then:

$$\mu_{CS} = \mu_{CF} \quad (19)$$

Where  $\mu_{CF}$  is the chemical potential of C in the contacting fluid. For a two-component system, A and C, the Gibbs-Duhem eqn. (15) shows:

$$n_{AS} d\mu_{AS} + n_{CS} d\mu_{CS} = n_{AS} d\mu_{AS} + n_{CS} d\mu_{CF} = 0 \quad (20)$$

So by changing the composition of the fluid phase in contact, the surface composition or the chemical potentials could be affected.

## The Stable Surface Layer

Which atoms should be enriched on the surface and form a stable layer? The usual finding is that the metal with lower surface energy or the larger atoms are enriched on the surface. Ma and Balbuena [20] collected data for some Pt<sub>3</sub>M systems and compared with their theoretical predictions with two notable exceptions, Pt<sub>3</sub>Mn {111} and Pt<sub>3</sub>Ti {111}. While their theory predicts Mn and Ti segregation, experiments showed Pt segregation [8,21]. So the surface segregation is governed, not by the atomic size mismatch and the surface energy differences but by the subsurface atomic arrangement, namely the shell structure. In other words, the shell free energy determines the surface composition.

Li et al. [22] discovered in the oxidative steam reforming of methane, a Pt coated Ni catalyst was better than a Pt-Ni alloy catalyst. Comparing to the activity in the steam reforming of methane without oxygen, the presence of oxygen led to decreased reforming activity in both pure Ni (2.6 wt% in catalyst) and Pt (0.1)+Ni (2.6) alloy due mainly to the oxidation of nickel, whereas Pt (0.1) coated over Ni (2.6) exhibited a high resistance to oxidation and maintained the activity even in the presence of oxygen. The mole ratio of Pt (0.1) to Ni (2.6) is only 0.01 and yet it was sufficient to protect Ni from oxidation. Considering the fact that the catalyst was calcined in air at 573 K for 3 hours and the bed temperature went as high as 1123 K in the oxidative steam reforming of methane we suspect that Pt segregates over the Ni surface and may not diffuse in as an alloy element.

Similarly Mukainakano et al. [23] found in the same steam reforming of methane, hysteresis with respect to the addition and removal of the methane oxygen mixture was clearly observed on a Pt (0.1)+Ni (2.6) alloy catalyst and pure Ni (2.6) catalyst but no hysteresis was observed for a Pt (0.1) coated Ni (2.6) catalyst. They also believed that the Pt coated Ni catalyst had Pt segregated on the surface which enhanced the reducibility of Ni drastically and eliminated the hysteresis behavior.

For steam reforming of ethanol, Soyal-Baltacioglu et al. [24] found the best catalyst was 0.3 wt% Pt-15 wt% Ni over  $\delta$ -Al<sub>2</sub>O<sub>3</sub>. Here the Pt/Ni atomic ratio was only 0.006. It shows the importance of understanding the surface enrichment rather than the surface excess.

## Pt-Shell Co-Core Nanoparticles

For Co core, Pt shell nanoparticles prepared by electroless deposition, Beard et al. [25] found that the lower Pt:Co ratio (monolayer Pt on Co) Pt-Co/C catalysts outperformed a commercial Pt/C catalyst.

Wang et al. [26] made ordered Pt<sub>3</sub>Co intermetallic particles coated with 2-3 atomic layers of Pt. These nanocatalysts exhibited over 200% increase in mass activity when compared with the disordered Pt<sub>3</sub>Co alloy nanoparticles.

So the monolayer Pt shell over Co nanowire is a distinct possibility. The size effect is shown by Frankenburg et al. [27]. Larger wires have better surfaces.

## Pt-Shell Pt-Cu Nanoparticles

Strasser et al. [28] made Pt<sub>25</sub>Cu<sub>75</sub>, Pt<sub>50</sub>Cu<sub>50</sub> and Pt<sub>75</sub>Cu<sub>25</sub> nano particles and annealed them at 800°C and 950°C and then dealloyed electrochemically to remove Cu from the surface. They found a Pt-enriched surface layer (about 0.6 nm thick) in all these 4 nm particles. The fcc unit cell parameter for Pt on the surface (0.388 nm for Pt<sub>75</sub>Cu<sub>25</sub>, 0.382 nm for Pt<sub>50</sub>Cu<sub>50</sub> and 0.375 nm for Pt<sub>25</sub>Cu<sub>75</sub>) was smaller than the

bulk Pt (0.392 nm) and they attributed the superb catalytic activity of these particles for the oxygen reduction reaction in fuel cell electrodes to the reduction in atomic spacing. For a thin layer of Pt on Cu the Pt spacing would be the smallest and the catalytic activity would be the best.

Yeh et al. [29] found that the oxygen reaction reactivity of the Pt-Cu nanorods was 2.2 times higher than that of the Pt nanoparticles after 1000 potential cycles. They attributed this to the 1-D morphology and the low Pt unfilled d-states by alloying.

### Pt Shell Ag Core Nanoparticles

Wojtysiak et al. [30] tried to cover Ag particles with Pt shell by the galvanic replacement reaction between Ag and  $\text{PtCl}_4^{2-}$ . However, the coverage was not good and the shell had a lot of holes. To improve the integrity of the shell, seeded growth of Pt on the surface of Ag by the reduction of  $\text{PtCl}_4^{2-}$  with ascorbic acid was used at room temperature. To cover the surface of an 11 nm Ag particle, the number of atoms of Pt in the final Ag@Pt core-shell particle must be at least the same as that of Ag.

Abkhalimov and Ershov [31] coated 6.3 nm Ag nanoparticles with Pt by treating with aqueous  $\text{K}_2\text{PtCl}_4$  with hydrogen. The Ag/Pt atomic ratio ranged from 1/9 to 9/1. They used these particles to catalyze the reduction of methyl viologen with hydrogen in an alkaline solution. They found a critical thickness of about 1 nm for Pt below which no catalysis will take place. This critical thickness can be reduced when the nanoparticles are replaced by nanowires of large diameters.

Pryadchenko et al. [32] made C supported PtAg nanoparticles by the chemical reduction of  $\text{H}_2\text{PtCl}_6$  and  $\text{AgNO}_3$  in a mixture of water: ethylene glycol=5:1. A 0.5 M  $\text{NaBH}_4$  solution was used as reducing agent. If both Ag and Pt salts were used together, the particles were solid solutions. But if the Ag salt was reduced first to form Ag nanoparticles and then Pt salt was added to be reduced, the nanoparticles had a core-shell structure. The shell had a thickness of at least 3 atomic layers of Pt.

### Pt Shell Ag Core Nanotubes

Kim et al. [33] made Ag nanowires by heating 20 mL ethylene glycol (EG) to 151.5 C and adding 4 mM  $\text{CuCl}_2 \cdot 2\text{H}_2\text{O}$  in 0.16 mL EG, 147 mM polyvinyl pyrrolidone (PVP, MW 55,000) in 6 mL EG, and 94 mM  $\text{AgNO}_3$  in 6 mL EG and maintaining at this temperature for one hr. resulting in a gray solution of Ag nanowires. See Korte et al. [34] for more details. To coat the Ag nano wires with Pt, the Ag nanowire solution (32.16 mL) was cooled to 100 C, added slowly 20 mM  $\text{K}_2\text{PtCl}_4$  in 6 mL EG and heated for 1 hr. The Pt shell Ag core nanotubes were obtained by centrifuge and washing several times with water and ethanol and  $\text{NH}_4\text{OH}$  to remove AgCl precipitates. To make pure Pt nanotubes, the Pt coated Ag nanotubes were treated with 6 M  $\text{HNO}_3$  solution to remove Ag. In alkaline media, the Pt coated Ag nanotubes showed 50% better activity than pure Pt nanotubes and Pt/C.

### Pt Shell Au Core Nanoparticles

Min et al. [35] overgrew Pt on the surface of Au nanocrystals of cubic, octahedral and spherical shapes. Different modes of overgrowth were observed depending on the shape of the gold core. It occurred on the planar surfaces of Au cubes, at the vertices of the Au octahedral and over the entire surface of the Au spheres.

Banerjee et al. [36] made 5 nm gold particles by the reduction of chloroauric acid with tannic acid and coated these particles by Pt using different amounts of chloroplatinic acid and hydrazine. For Pt/Au

ratios of 0.19, 0.39, 0.58 and 0.88, the Pt thickness was half a monolayer, 1, 1.5 and 2 monolayers, respectively. The electrochemical activity was the best for the 2 monolayers with a mass activity 3 times better than the pure Pt nanoparticles.

Roy et al. [37] used 40 nm Au nanocrystals with extensive {111} facets and deposited 5 atomic layers of Pt on the surface by reducing hexachloroplatinic acid with ascorbic acid. Electrochemical evaluations revealed a compact Pt shell with a mass activity 4 times better than Pt black and comparable to that of Pt bulk metal.

Hartl et al. [38] used commercial 30 nm Au particles, highly crystalline and stably dispersed. To the dispersion they added hexachloroplatinic acid (mass of Pt=20% of Au), heated to 70-80°C, added 0.01 M ascorbic acid to reduce Pt to coat on Au particles. The Pt shell was about 3 atomic layers thick. The electrocatalytic activity for the oxygen reduction reaction using these core-shell particles equals that of bulk Pt.

Xiao et al. [39] fabricated nanoporous film of 100 nm thick by dealloying  $\text{Au}_{50}\text{Ag}_{50}$  leaf at room temperature for 8 hours, rinsed and treated with 0.31 mM  $\text{H}_2\text{PtCl}_6$  and 0.13 mM  $\text{HCOOH}$  in the dark to deposit Pt on Au. The catalytic activity of the nanoporous AuPt film towards electrochemical oxidation of methanol increases with the loading level of Pt, resulting in the highest electrochemical area of 70.4  $\text{m}^2/\text{g}$  Pt, about 3 monolayers. Compared to the Pt nanoparticles supported in C, this self-supporting film uses much less Pt.

Kulp et al. [40] made Au nanoparticles by adding 1 mL of 1 wt% solution of  $\text{HAuCl}_4 \cdot 3\text{H}_2\text{O}$  to 250 mL water with vigorous stirring. Then 1 mL of 1 wt%  $\text{Na}_3\text{C}_6\text{H}_5\text{O}_7 \cdot 2\text{H}_2\text{O}$  in water was added and after 1 min, 1 mL of 1 wt%  $\text{NaBH}_4$  and 1 wt% of  $\text{Na}_3\text{C}_6\text{H}_5\text{O}_7 \cdot 2\text{H}_2\text{O}$  was added. The color change of the solution from light yellow to orange red indicated the formation of Au nanoparticles. The solution was stirred for another 10 min followed by adding 90 mg of Vulcan XC72 with continued stirring for 45 more min. The solution was filtered yielding a clear colorless filtrate which was dried for 3 hours at 90°C. TEM images showed homogeneously distributed colorless Au particles of about 5.5 nm adsorbed on C. To coat Pt shells on these particles, they used glassy carbon electrode in a solution of Pt ( $\text{NO}_3$ )<sub>2</sub> and  $\text{NaNO}_3$  by pulsed electro deposition. See paper for details.

Zhang et al. [41] coated 6 nm Au particles with Pt resulting in particles of  $9.0 \pm 2.4$  nm,  $10.4 \pm 2.8$  nm and  $13.0 \pm 3.2$  nm sizes. These particles stabilized by polyaryl ether trisacetic acid ammonium chloride dendrons and had higher catalytic activity than monometallic Pt nanoparticles. They attributed this to the fact that Au core attracts electrons from Pt.

Li et al. [42] made 55 nm Au particles by reducing  $\text{AuCl}_4^-$  with sodium citrate. Then different amounts of 1 mM of  $\text{H}_2\text{PtCl}_6$  were added and the mixture was heated to 80°C. Then while stirring, a solution of 10 mM of ascorbic acid was slowly dropped into the mixture until half of the volume of  $\text{H}_2\text{PtCl}_6$  was added. The mixture was stirred for another 30 min. and should change from red brown to dark brown indicating the coating was complete. The final diameter of the core-shell particle can be estimated from the volume ratios of Au and Pt. The mixture was then centrifuged 3 times before coated on a smooth and clean glass carbon surface for testing.

Gao et al. [43] coated only 2 monolayers of Pt on 16 nm Au particles by reducing  $\text{H}_2\text{PtCl}_6$  with ascorbic acid. The uncoated Au nanoparticles exhibited a strong localized surface Plasmon resonance (LSPR) peak at 520 nm. After coating, the LSPR peak shifted to 508 nm.



Zhang et al. [44] made 55 nm Au particles by reducing  $\text{HAuCl}_4$  with sodium citrate. Then 30 mL of sol containing the 55 nm Au seeds were mixed with 0.76 mL of 1 mM  $\text{H}_2\text{PtCl}_4$  and heated to 80°C for a few minutes. Ascorbic acid (0.4 mL, 10 mM) was slowly dropped into the mixture with vigorous stirring. The coated Pt shell over the Au surface was about 0.7 nm thick. The coated Au particles were almost spherical. The sol was centrifuged 3 times to remove excess reactants.

From these observations, it seems likely that gold wires can be coated with only one mono layer of Pt to increase its catalytic activity.

### Pt and Pt Alloy Nanowires

Higgins et al. [45] made Pt-Co alloy nanowires by mixing 0.001 M Pt acetylacetonate and 0.001 M Co carbonyl, dissolved in ethylenediamine under nitrogen protection and transferred to an autoclave reactor at 160°C for 1 hour under 600 W powers. Pt-Co alloy nanowires of about 35-60 nm diameters were formed and collected by filtration and washing followed by annealing at 600°C in Ar for 1 hr. These nanowires were found much more stable catalytically than Pt nanoparticles supported on C.

Yaipimai and Pornprasertsuk [46] made Pt, Pt-Cu and Pt-Sn alloy nanowires by electro spinning using the salts and PVP, Poly (vinyl pyrrolidone) with molecular weights  $1.3 \times 10^6$  and  $4 \times 10^4$  g/mole.

### Pt Shell Pd Core Nanoparticles

Cao et al. [47] made the Pd core Pt shell nanoparticles by using an area selective atomic layer deposition method. The Pt shell thickness could be monitored by an in-situ quartz crystal microbalance. The catalyst with one monolayer Pt shell showed the best mass activity and selectivity and the lowest barrier for CO oxidation.

Choi et al. [48] did electro less deposition of Cu on Pd Nanoparticles and galvanic displacement of Cu by Pt. The catalyst is active toward electro-oxidation of methanol and is more stable against CO poisoning than a commercial Pt/C catalyst.

D'Souza and Sampath [49] made highly uniform, stable Nano bimetallic dispersions using organically modified silicates as the matrix and the stabilizer. They found that the structure of the particles consists of a Pt shell and a Pd core. No aggregation or segregation of the particles was observed after prolonged storage of several months.

Shao et al. [50] found that the specific oxygen reduction reaction activity of Pt shells over Pd octahedra enriched with {111} facets was 28 times higher than that of Pd octahedra without Pt. It was only 3 times better than Pt coated Pd cubes enriched with {100} facets. The Pt coated Pd octahedra also showed excellent durability during potential cycling suggesting their great potential for application in fuel cells.

Wongkaew et al. [51] made electro less deposition of Pt on Pd surfaces of 30 wt% Pd/C. Pt loadings of 6.0, 11.7, 17.2 and 22.7 wt% corresponded to Pt shells of 0.9, 1.7, 2.7 and 3.4 monolayers on Pd. These core/shell catalysts were very active, especially the sample of 0.9 monolayer coverage which had a mass activity of 329 A/gPt as compared to 183 A/gPt for a conventional 50.5 wt% Pt/C sample.

Li et al. [52] synthesized C supported  $\text{Pd}_3\text{Au}@\text{Pt}$  core-shell electrocatalyst by chemical reduction of  $\text{K}_2\text{PtCl}_4$ ,  $\text{K}_2\text{PdCl}_4$  and  $\text{NaAuCl}_4$  with ascorbic acid. The resultant particles (3.4 nm diameter core) had a thin layer (less than 1 nm) of Pt shell. They had a mass activity of 939 A/gPt for oxygen reduction reaction, 4.6 times that of commercial Pt/C (203 A/gPt). But the durability was about the same. They proposed that

the tension in the Pt shell and the electron transfer from the core to the shell contributed to the improved electrocatalytic activity.

### Pt Shell Ru Core Nanoparticles

Chen et al. [53] coated Ru nanoparticles (3.2 nm diameter) with 1.5-3.6 atomic layers of Pt. The sample with 1.5 atomic layers showed a 3.2 fold improvement in CO tolerance and 2.4 fold current enhancements during methanol oxidation as compared to the commercial Pt/C.

Yang et al. [54] found that the Pt shell grew on <111> radial facets and <200> face facets of the Ru core if the incubation time was short. For 2 hours incubation, severe chemical etching occurred prior to shell growth. So the dynamic rearrangement at the core-shell interface is important for the final structure.

Wang et al. [55] made Pt shell (0.42 nm thick or about 1.5 atomic layers) and Ru core (3.18 nm diameter) nanoparticles (4.02 nm diameter total). Compared to the pure Pt nanoparticles of 4.38 nm diameter, these Pt-shell Ru-core nanoparticles showed 4.5 fold more power density for the direct methanol fuel cell. The open circuit voltage was improved by 0.18 V (from 0.49 to 0.67 V). They attribute the improvement to the lattice compression in the Pt shell due to the core.

Huang et al. [56] made 15 wt%  $\text{Pt}_{50}\text{Ru}_{50}/\text{C}$  nano particles (2 nm) by the method of incipient wetness impregnation and activated by hydrogen reduction at 620 K. The reduced catalyst with Pt rich in the shell and Ru rich in the core was subsequently modified by oxidation in air. This oxidation enhanced significantly the electrochemical activity of Pt-Ru/C for electro-oxidation of methanol. Such enhancement was attributed to the segregation of Ru and the formation of  $\text{RuO}_2$ .

### Pt Shell Pd Core Nanowires

Guo et al. [57] started with Te nanowires (11 nm diameter) produced by a hydrothermal route and used them as both reducing agent and sacrificial template to make Pd nanowires in aqueous solution at room temperature in less than 5 min. The Pd nanowires were used as seeds to direct dendritic growth of Pt upon the reduction of  $\text{K}_2\text{PtCl}_4$  with ascorbic acid in aqueous solution.

Liao and Hou [58] made Pt-on- $\text{Pd}_{0.85}\text{Bi}_{0.15}$  nanowires by a facile, one pot, wet-chemical and templateless method in the presence of oleylamine and  $\text{NH}_4\text{Br}$ . These nanowires had  $8.3 \pm 1.1$  nm diameters and  $387 \pm 105$  nm length. Small Pt nanobranches (5 nm) grew on the Pd nanowires at the end of which Pt nanoflowers grew. They could see also about 2 nm thick of amorphous C on the nanowires. Depending on the composition and the ratio of Pd/Bi/Pt they could grow nanowires, nanoflowers, nanoparticles or nanoplates. They all demonstrated high electro-chemical activity and durability for the oxygen reduction reaction.

Xia et al. [59] reported a facile solvothermal synthesis of nanowire assemblies composed of ultra-thin (3 nm) and ultra-long (10  $\mu\text{m}$ ) Pt, Pt-Au and Pt-Pd nanowires without involving any template. These nanowires can be easily cast into a free-standing membrane which exhibits excellent electro catalytic activity and very high stability for formic acid and methanol oxidation and the oxidation reduction reaction.

### Pt Shell Cu Core Networks

Feng et al. [60] made nanoporous Cu by electrodepositing Zn on a 0.1 mm Cu plate, making Cu-Zn alloy by heating and then removing Zn by HCl. They followed the method described by Leaman [61].

Then they deposited Pt onto the Cu surfaces by electroless plating. This NPCu-Pt catalyst can reduce CO<sub>2</sub> in the ionic liquid BMIMBF<sub>4</sub> (1-butyl-3-methyl-imidazolium-tetra-fluoborate) with more stable current, higher current density and efficiency compared to the pure Pt catalyst.

### Pt Shell Cu Core Nanowires

Alia et al. [62] and Wittkopf et al. [63] already made Pt shell (14 monolayers) over Cu core nano wires with mass activities of 0.1-1.0 A/mgPt which may be improved by reducing the number of monolayers of Pt on the surface.

### Conclusions

It is seen that there are many possibilities to make a single layer Pt Shell over large nanowires of a cheaper metal so a commercial catalyst for a fuel cell can be made to make self-driving automobiles widely used soon. It is anticipated that we will have cheaper and safer ground transportation available in the very near future.

### References

- Ugurlu A, Oztuna S (2015) A comparative analysis study of alternative energy sources for automobiles. *International Journal of Hydrogen Energy* 40: 11178-11188.
- Zhu XH, Chen JY, Zhong MR (2015) Dynamic interacting relationships among international oil prices, macroeconomic variables and precious metal prices. *Transactions of Nonferrous Metals Society of China* 25: 669-676.
- Gauthier Y, Joly Y, Baudoing R, Rundgren J (1985) Surface-sandwich segregation on nondilute bimetallic alloys: Pt 50 Ni 50 and Pt 78 Ni 22 probed by low-energy electron diffraction. *Physical Review B* 31: 6216.
- Gauthier Y, Baudoing-Savois R, Rundgren J, Hammar M, Gothelid M (1995) Reconstruction of the Pt50Ni50 (100) surface: A LEED and STM study. *Surface Science* 327: 100-120.
- Van de Riet EGJP, Deckers S, Habraken FHPM, Niehaus A (1991) The atomic surface structure of Pt0.5Ni0.5 (111). *Surface Science* 243: 49-57.
- Wang G, Van Hove MA, Ross PN, Baskes MI (2005) Quantitative prediction of surface segregation in bimetallic Pt-M alloy nanoparticles (M=Ni, Re, Mo). *Progress in Surface Science* 79: 28-45.
- Stamenkovic VR, Fowler B, Mun BS, Wang G, Ross PN, et al. (2007) Improved oxygen reduction activity on Pt3Ni (111) via increased surface site availability. *Science* 315: 493-497.
- Gallego S, Ocal C, Munoz MC, Soria F (1997) Surface-layered ordered alloy (Pt/Pt3Mn) on Pt (111). *Physical Review B* 56: 12139.
- Shui JL, Zhang JW, Li JC (2011) Making Pt-shell Pt 30 Ni 70 nanowires by mild dealloying and heat treatments with little Ni loss. *Journal of Materials Chemistry* 21: 6225-6229.
- De Temmerman L, Creemers C, Van Hove H, Neyens A, Bertolini JC, et al. (1986) Experimental determination of equilibrium surface segregation in Pt-Ni single crystal alloys. *Surface Science* 178: 888-896.
- Gauthier Y, Hoffmann W, Wuttig M (1990) Structure and composition of Pt10Ni90 (100): A low energy electron diffraction study. *Surface Science* 233: 239-247.
- Hebenstreit W, Ritz G, Schmid M, Biedermann A, Varga P (1997) Segregation and reconstructions of Pt<sub>x</sub>Ni<sub>1-x</sub> (100). *Surface Science* 388: 150-161.
- Godínez-Salomón F, Hallen-López M, Solorza-Feria O (2012) Enhanced electroactivity for the oxygen reduction on Ni@Pt core-shell nanocatalysts. *International Journal of Hydrogen Energy* 37: 14902-14910.
- Jung N, Chung YH, Chung DY, Choi KH, Park HY, et al. (2013) Chemical tuning of electrochemical properties of Pt-skin surfaces for highly active oxygen reduction reactions. *Physical Chemistry Chemical Physics* 15: 17079-17083.
- Kang J, Wang R, Wang H, Liao S, Key J, et al. (2013) Effect of Ni core structure on the electrocatalytic activity of Pt-Ni/C in methanol oxidation. *Materials* 6: 2689-2700.
- Shui J, Li JC (2009) Platinum nanowires produced by electrospinning. *Nano Letters* 9: 1307-1314.
- Ikeda H, Qi Y, Cagin T, Samwer K, Johnson WL, et al. (1999) Strain rate induced amorphization in metallic nanowires. *Physical Review Letters* 82: 2900.
- Serrà A, Gómez E, Vallés E (2015) Novel electrodeposition media to synthesize CoNi-Pt Core@Shell stable mesoporous nanorods with very high active surface for methanol electro-oxidation. *Electrochimica Acta* 174: 630-639.
- Tao F, Grass ME, Zhang Y, Butcher DR, Renzas JR, et al. (2008) Reaction-driven restructuring of Rh-Pd and Pt-Pd core-shell nanoparticles. *Science* 322: 932-934.
- Ma Y, Balbuena PB (2008) Pt surface segregation in bimetallic Pt 3 M alloys: a density functional theory study. *Surface Science* 602: 107-113.
- Chen W, Severin L, Göthelid M, Hammar M, Cameron S, et al. (1994) Electronic and geometric structure of clean Pt 3 Ti (111). *Physical Review B* 50: 5620.
- Li B, Kado S, Mukainakano Y, Miyazawa T, Miyao T, et al. (2007) Surface modification of Ni catalysts with trace Pt for oxidative steam reforming of methane. *Journal of Catalysis* 245: 144-155.
- Mukainakano Y, Yoshida K, Kado S, Okumura K, Kunimori K, et al. (2008) Catalytic performance and characterization of Pt-Ni bimetallic catalysts for oxidative steam reforming of methane. *Chemical Engineering Science* 63: 4891-4901.
- Soyal-Baltacıoğlu F, Aksoyulu AE, Önsan ZI (2008) Steam reforming of ethanol over Pt-Ni Catalysts. *Catalysis Today* 138: 183-186.
- Beard KD, Borrelli D, Cramer AM, Blom D, Van Zee JW, et al. (2009) Preparation and structural analysis of carbon-supported Co core/Pt shell electrocatalysts using electroless deposition methods. *ACS Nano* 3: 2841-2853.
- Wang D, Xin HL, Hovden R, Wang H, Yu Y, et al. (2013) Structurally ordered intermetallic platinum-cobalt core-shell nanoparticles with enhanced activity and stability as oxygen reduction electrocatalysts. *Nature Materials* 12: 81-87.
- Frankenburg WG, Komarewsky VI, Rideal EK (1952) *Advances in catalysis* (Vol. 4). Academic Press.
- Strasser P, Koh S, Annyev T, Greeley J, More K, et al. (2010) Lattice-strain control of the activity in dealloyed core-shell fuel cell catalysts. *Nature Chemistry* 2: 454-460.
- Yeh TH, Liu CW, Chen HS, Wang KW (2013) Preparation of carbon-supported PtM (M=Au, Pd, or Cu) nanorods and their application in oxygen reduction reaction. *Electrochemistry Communications* 31: 125-128.
- Wojtyśiak S, Solla-Gullón J, Dłuzewski P, Kudelski A (2014) Synthesis of core-shell silver-platinum nanoparticles, improving shell integrity. *Colloids and Surfaces A: Physicochemical and Engineering Aspects* 441: 178-183.
- Abkhalimov EV, Ershov BG (2014) The size effect in the catalytic activity of AgcorePtshell nanoparticles. *Colloid Journal* 76: 381-386.
- Pryadchenko VV, Srabionyan VV, Mikheykina EB, Avakyan LA, Murzin VY, et al. (2015) Atomic Structure of Bimetallic Nanoparticles in PtAg/C Catalysts: Determination of Components Distribution in the Range from Disordered Alloys to "Core-Shell" Structures. *The Journal of Physical Chemistry C* 119: 3217-3227.
- Kim Y, Kim H, Kim WB (2014) PtAg nanotubes for electrooxidation of ethylene glycol and glycerol in alkaline media. *Electrochemistry Communications* 46: 36-39.
- Korte KE, Skrabalak SE, Xia Y (2008) Rapid synthesis of silver nanowires through a CuCl<sub>2</sub>-or CuCl<sub>2</sub>-mediated polyol process. *Journal of Materials Chemistry* 18: 437-441.
- Min M, Kim C, Yang YI, Yi J, Lee H (2009) Surface-specific overgrowth of platinum on shaped gold nanocrystals. *Physical Chemistry Chemical Physics* 11: 9759-9765.
- Banerjee I, Kumaran V, Santhanam V (2015) Synthesis and characterization of Au@Pt nanoparticles with ultrathin platinum overlayers. *The Journal of Physical Chemistry C* 119: 5982-5987.
- Roy RK, Njagi JI, Farrell B, Halaciuga I, Lopez M, et al. (2012) Deposition of continuous platinum shells on gold nanoparticles by chemical precipitation. *Journal of Colloid and Interface Science* 369: 91-95.
- Hartl K, Mayrhofer KJ, Lopez M, Goia D, Arenz M (2010) AuPt core-shell

- nanocatalysts with bulk Pt activity. *Electrochemistry Communications* 12: 1487-1489.
39. Xiao S, Xiao F, Hu Y, Yuan S, Wang S, et al. (2014) Hierarchical nanoporous gold-platinum with heterogeneous interfaces for methanol electrooxidation. *Scientific Reports*, p: 4.
  40. Kulp C, Chen X, Puschhof A, Schwamborn S, Somsen C, et al. (2010) Electrochemical synthesis of core-shell catalysts for electrocatalytic applications. *ChemPhysChem* 11: 2854-2861.
  41. Zhang W, Li L, Du Y, Wang X, Yang P (2009) Gold/platinum bimetallic core/shell nanoparticles stabilized by a fréchet-type dendrimer: Preparation and catalytic hydrogenations of phenylaldehydes and nitrobenzenes. *Catalysis Letters* 127: 429-436.
  42. Li JF, Yang ZL, Ren B, Liu GK, Fang PP, et al. (2006) Surface-enhanced Raman spectroscopy using gold-core platinum-shell nanoparticle film electrodes: toward a versatile vibrational strategy for electrochemical interfaces. *Langmuir* 22: 10372-10379.
  43. Gao Z, Tang D, Tang D, Niessner R, Knopp D (2015) Target-induced nanocatalyst deactivation facilitated by core@ shell nanostructures for signal-amplified headspace-colorimetric assay of dissolved hydrogen sulfide. *Analytical Chemistry* 87: 10153-10160.
  44. Zhang P, Cai J, Chen YX, Tang ZQ, Chen D, et al. (2009) Potential-dependent chemisorption of carbon monoxide at a gold core-platinum shell nanoparticle electrode: A combined study by electrochemical in situ surface-enhanced Raman spectroscopy and density functional theory. *The Journal of Physical Chemistry C* 114: 403-411.
  45. Higgins DC, Ye S, Knights S, Chen Z (2012) Highly durable platinum-cobalt nanowires by microwave irradiation as oxygen reduction catalyst for PEM fuel cell. *Electrochemical and Solid-State Letters* 15: B83-B85.
  46. Yaipimai W, Pomprasertsuk R (2013) Fabrication of Pt, Pt-Cu, and Pt-Sn nanofibers for direct ethanol protonic ceramic fuel cell application. *Journal of Materials Science* 48: 4059-4072.
  47. Cao K, Liu X, Zhu Q, Shan B, Chen R (2015) Atomically Controllable Pd@ Pt Core-Shell Nanoparticles towards Preferential Oxidation of CO in Hydrogen Reactions Modulated by Platinum Shell Thickness. *ChemCatChem*.
  48. Choi I, Ahn SH, Kim MH, Kwon OJ, Kim JJ (2014) Synthesis of an active and stable Pt shell-Pd core/C catalyst for the electro-oxidation of methanol. *International Journal of Hydrogen Energy* 39: 3681-3689.
  49. D'Souza L, Sampath S (2000) Preparation and Characterization of Silane-Stabilized, Highly Uniform, Nanobimetallic Pt-Pd Particles in Solid and Liquid Matrixes. *Langmuir* 16: 8510-8517.
  50. Shao M, He G, Peles A, Odell JH, Zeng J, et al. (2013) Manipulating the oxygen reduction activity of platinum shells with shape-controlled palladium nanocrystal cores. *Chemical Communications* 49: 9030-9032.
  51. Wongkaew A, Zhang Y, Tengco JMM, Blom DA, Sivasubramanian P, et al. (2016) Characterization and evaluation of Pt-Pd electrocatalysts prepared by electroless deposition. *Applied Catalysis B: Environmental* 188: 367-375.
  52. Li H, Yao R, Wang D, He J, Li M, Song Y (2015) Facile Synthesis of Carbon Supported Pd<sub>3</sub>Au@ Super-Thin Pt Core/Shell Electrocatalyst with a Remarkable Activity for Oxygen Reduction. *The Journal of Physical Chemistry C* 119: 4052-4061.
  53. Chen TY, Lin TL, Luo TJM, Choi Y, Lee JF (2010) Effects of Pt Shell Thicknesses on the Atomic Structure of Ru-Pt Core-Shell Nanoparticles for Methanol Electrooxidation Applications. *ChemPhysChem* 11: 2383-2392.
  54. Yang PW, Liu YT, Hsu SP, Wang KW, Jeng US, et al. (2015) Core-shell nanocrystallite growth via heterogeneous interface manipulation. *CrytEngComm* 17: 8623-8631.
  55. Wang JJ, Liu YT, Chen IL, Yang YW, Yeh TK, et al. (2014) Near-Monolayer Platinum Shell on Core-Shell Nanocatalysts for High-Performance Direct Methanol Fuel Cell. *The Journal of Physical Chemistry C* 118: 2253-2262.
  56. Huang SY, Chang SM, Lin CL, Chen CH, Yeh CT (2006) Promotion of the electrochemical activity of a bimetallic platinum-ruthenium catalyst by oxidation-induced segregation. *The Journal of Physical Chemistry B* 110: 23300-23305.
  57. Guo S, Dong S, Wang E (2010) Ultralong Pt-on-Pd bimetallic nanowires with nanoporous surface: nanodendritic structure for enhanced electrocatalytic activity. *Chemical Communications* 46: 1869-1871.
  58. Liao H, Hou Y (2013) Liquid-phase templateless synthesis of Pt-on-Pd<sub>0</sub>. 85Bi<sub>0</sub>. 15 nanowires and PtPdBi porous nanoparticles with superior electrocatalytic activity. *Chemistry of Materials* 25: 457-465.
  59. Xia BY, Wu HB, Yan Y, Lou XW, Wang X (2013) Ultrathin and ultralong single-crystal platinum nanowire assemblies with highly stable electrocatalytic activity. *Journal of the American Chemical Society* 135: 9480-9485.
  60. Feng Q, Liu S, Wang X, Jin G (2012) Nanoporous copper incorporated platinum composites for electrocatalytic reduction of CO<sub>2</sub> in ionic liquid BMIMBF<sub>4</sub>. *Applied Surface Science* 258: 5005-5009.
  61. Leaman FH (1972) US Patent 3698939.
  62. Alia SM, Jensen K, Contreras C, Garzon F, Pivovar B, et al. (2013) Platinum coated copper nanowires and platinum nanotubes as oxygen reduction electrocatalysts. *Acs Catalysis* 3: 358-362.
  63. Wittkopf JA, Zheng J, Yan Y (2014) High-performance dealloyed PtCu/CuNW oxygen reduction reaction catalyst for proton exchange membrane fuel cells. *Acs Catalysis* 4: 3145-3151.

Citation: Li JCM (2017) Pt-Shell Nanowires for Fuel Cell Electrodes. J Material Sci Eng 6: 337. doi: [10.4172/2169-0022.1000337](https://doi.org/10.4172/2169-0022.1000337)

### OMICS International: Open Access Publication Benefits & Features

#### Unique features:

- Increased global visibility of articles through worldwide distribution and indexing
- Showcasing recent research output in a timely and updated manner
- Special issues on the current trends of scientific research

#### Special features:

- 700+ Open Access Journals
- 50,000+ Editorial team
- Rapid review process
- Quality and quick editorial, review and publication processing
- Indexing at major indexing services
- Sharing Option: Social Networking Enabled
- Authors, Reviewers and Editors rewarded with online Scientific Credits
- Better discount for your subsequent articles

Submit your manuscript at: <http://www.omicsgroup.org/journals/submit>